Philippine Engineering Journal (1999) XX (2): 32-42

INCREASE IN THE DYNAMIC FORCE TRANSMITTED BY A MASS-SPRING-DAMPER SYSTEM MODEL

Jaime Y. Hernandez, Jr.[1] and William Tanzo, DEng.[2]

[1]Assistant Professor
Department of Engineering Sciences
College of Engineering
University of the Philippines
Diliman, Quezon City Philippines

[2]Associate Professor
Department of Civil Engineering
University of the Philippines
Los Banos, Laguna, Philippines

ABSTRACT

The analysis of a mass-spring-damper system model shows a variation in the derived equation of the dynamic force transmitted compared to that of the applied force when the model is subjected to a sinusoidal displacement load. Upon substitution of values, the force-time history plot shows a possible increase in the transmitted force. This can be seen as the tilting of the principal axis of the corresponding hysteresis loop which implies an increase in stiffness. This phenomenon was observed during the testing of the LOAD DISTRIBUTION and ENERGY-DISSIPATING (LDED) device. The LDED device is effective in transmitting structure generated forces while dissipating a portion of the energy induced during earthquakes.

I. Introduction

The mass-spring damper system has been extensively used in modeling single-degree-of-freedom and multi-degree-of-freedom systems in civil engineering when considering structural response to dynamic motion. The mass, assumed to be rigid, represents the mass of the system under consideration. The linear spring represents the stiffness of the system while the viscous damper corresponds to the inherent capability of the system to dissipate energy. Although the current emphasis on most research work is on modeling the behavior of inelastic systems, the mass-spring-damper system with its inherent assumption of linear behavior has proven to be an effective tool in developing principles and explaining physical behavior of systems subjected to dynamic loading.

In this paper a mass-spring-damper system model subjected to a sinusoidal displacement load was analyzed - the equation of the transmitted force at steady-state condition was derived. This formula was compared with the derived equation for the applied force on the other end of the model. The force-time history plot shows an amplification of the transmitted force, and the hysteresis loop shows an increase in stiffness.

This phenomenon was observed during the testing of the LOAD DISTRIBUTION and ENERGY-DISSIPATING (LDED) device. The LDED device is a special form of energy-dissipating device because it not only dissipates a significant amount of energy from the structure but also enhances the lateral load distribution of earthquake generated forces by effecting load sharing among the substructure components. This dual function is made possible because of the

two major components of this device, namely: 1. the stiffening component which consists of a piston inside a cylinder housing filled with silicone putty - a material which easily deforms under slow loading but hardens when subjected to high-frequency loads, and 2. the damping component consisting of high-damping rubber vulcanized in-between two metal cylinders.

2. Analysis of Mass-Spring-Damper System Model

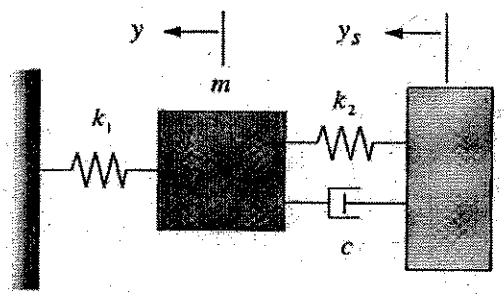

Figure 1. Mass-Spring-Damper System Model

Figure 1 shows the mass-spring-damper system model, it consists of a central mass *m*, a spring of stiffness k_1 on the left end of the mass and a spring of stiffness k_2 and a damper with damping c (in parallel) on the right end of the mass. Another body applies the sinusoidal displacement loading on the model.

It is the steady-state response of the model that is of interest. Specifically, the transmitted dynamic force to the fixed support. First the model was analyzed as shown - Model Case 1, the equation of the steady-state transmitted force was determined. In order to determine the steady-state response on the other end of the model, the model was reversed - Model Case 2.

Model Case 1

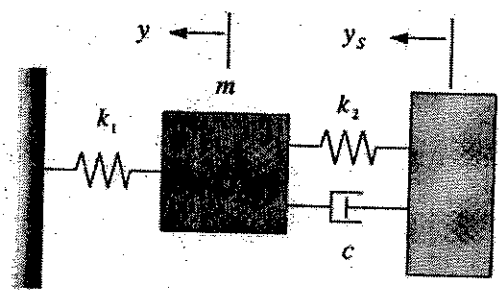

Figure 2. Mass-Spring-Damper System Model

The free-body diagram of mass m,

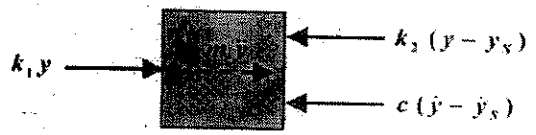

Figure 3. Free-Body Diagram of mass m

Summation of forces yields,

(1) $$m\ddot{y} - c(\dot{y} - \dot{y}_s) - k_2 (y - y_s) + k_1 y = 0$$

(2) $$m\ddot{y} - c\dot{y} - (k_2 - k_1) y = -(c\dot{y}_s + k_2 y_s)$$

Noting that $y_s(t) = y_0 \sin \varpi t$ and therefore $\dot{y}_s(t) = \varpi y_0 \cos \varpi t$

(3) $$m\ddot{y} - c\dot{y} - (k_2 - k_1)y = -(c\varpi y_0 \cos \varpi t + k_2 y_0 \sin \varpi t)$$

Equation 3 can be simplified into,

(4) $$m\ddot{y} - c\dot{y} - (k_2 - k_1)y = F_0 \sin(\varpi t + \beta)$$

where,

$$\tan \beta = \frac{c\varpi}{k_2}$$

$$F_0 = -y_0 \sqrt{(c\varpi)^2 + (k_2)^2}$$

Because of displacement controlled loading, we are only interested in the steady-state response of the model. This is determined by solving for the particular solution y_p of equation 4.

Assume

$$y_p(t) = C_1 \sin \varpi t + C_2 \cos \varpi t$$

If we use

$$e^{i\varpi t} = \cos \varpi t + i \sin \varpi t$$

then equation 4 becomes,

(5) $$m\ddot{y} - c\dot{y} - (k_2 - k_1)y = F_0 e^{i(\varpi t + \beta)}$$

$$y_p = C e^{i(\varpi t+\beta)}$$

(6)
$$\dot{y}_p = Ci\,\varpi\, e^{i(\varpi t+\beta)}$$

$$\ddot{y}_p = -C\varpi^2 e^{i(\varpi t+\beta)}$$

Substituting equations 6 into equation 5,

$$-mC\varpi^2 - ci\varpi\, C - (k_2 - k_1)C = F_0$$

(7)
$$C = \frac{-F_0}{m\varpi^2 + ic\varpi + (k_2 - k_1)}$$

Therefore,

(8)
$$y_p = \frac{-F_0 e^{i(\varpi t+\beta)}}{m\varpi^2 + (k_2 - k_1) + ic\varpi}$$

By using polar coordinates, this equation can be expressed in trigonometric form. Taking only the imaginary part of the solution,

(9)
$$y_p = \frac{F_0 \sin(\varpi t + \beta - \theta_1)}{\sqrt{[m\varpi^2 + (k_2 - k_1)]^2 + (c\varpi)^2}}$$

where,

$$\tan\theta_1 = \frac{c\varpi}{m\varpi^2 + (k_2 - k_1)}$$

Therefore, the steady-state solution is,

(10)
$$y_p = Y_1 \sin(\varpi t + \beta - \theta_1)$$

where,

$$Y_1 = \frac{y_0\sqrt{(c\varpi)^2 + (k_2)^2}}{\sqrt{[m\varpi^2 + (k_2 - k_1)]^2 + (c\varpi)^2}}$$

The force transmitted to the support, considering steady-state response is,

$$f_T = f_s = k_1 y_p$$

(11)
$$= k_1 Y_1 \sin(\varpi t + \beta - \theta_1)$$

with the maximum value of $f_T(t)$ over time as,

$$(f)_{T0} = k_1 Y_1 = \frac{k_1 y_0 \sqrt{(c\varpi)^2 + (k_2)^2}}{\sqrt{[m\varpi^2 + (k_2 - k_1)]^2 + (c\varpi)^2}} \tag{12}$$

Model Case 2

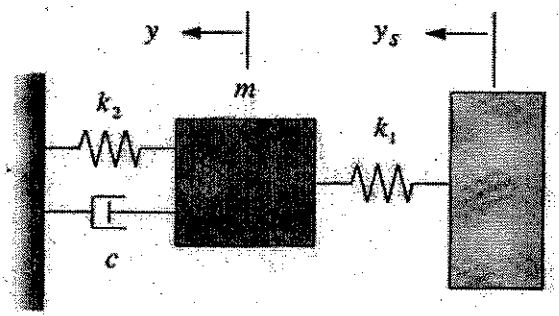

Figure 4. Reversed Mass-Spring-Damper System Model

The free-body diagram of mass m,

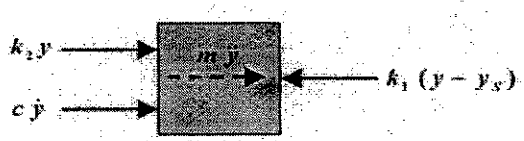

Figure 5. Free-Body Diagram of mass m

Summation of forces yields,

$$m\ddot{y} + c\dot{y} + k_2 y - k_1(y - y_s) = 0 \tag{13}$$

$$m\ddot{y} + c\dot{y} + (k_2 - k_1)y = -k_1 y_s = -k_1 y_0 \sin \varpi t \tag{14}$$

Recalling that $e^{i\varpi t} = \cos \varpi t + i \sin \varpi t$, equation 14 can be expressed as

$$m\ddot{y} + c\dot{y} + (k_2 - k_1)y = -k_1 y_0 \, e^{i\varpi t} \tag{15}$$

After substituting $y_p = Ce^{i\varpi t}$ into equation 15 and simplifying, we get

$$-mC\varpi^2 + ci\varpi C + (k_2 - k_1)C = -k_1 y_0$$

(16)
$$C = \frac{-k_1 y_0}{-m\varpi^2 + ic\varpi + (k_2 - k_1)}$$

Therefore,

(17)
$$y_p = \frac{-k_1 y_0 e^{i\varpi t}}{(k_2 - k_1) - m\varpi^2 + ic\varpi}$$

Again by using polar coordinates, this equation can be expressed in trigonometric form. Taking only the imaginary part of the solution,

(18)
$$y_p = \frac{k_1 y_0 \sin(\varpi t + \theta_2)}{\sqrt{[(k_2 - k_1) - m\varpi^2]^2 + (c\varpi)^2}}$$

where,

$$\tan\theta_2 = \frac{c\varpi}{m\varpi^2 - (k_2 - k_1)}$$

Therefore, the steady-state solution is,

(19)
$$y_p = Y_2 \sin(\varpi t + \theta_2)$$

where,
$$Y_2 = \frac{k_1 y_0}{\sqrt{[(k_2 - k_1) - m\varpi^2]^2 + (c\varpi)^2}}$$

Noting that tan (-θ) = -tan θ, we can express the particular solutions as,

(20)
$$y_p = Y_2 \sin(\varpi t - \theta_2)$$

where,

$$\tan\theta_2 = \frac{c\varpi}{(k_2 - k_1) - m\varpi^2}$$

The force transmitted to the support, considering steady-state response is,

$$g_T = f_s + f_D = k_2 y_p + c\dot{y}_p$$

$$= k_2 Y_2 \sin(\varpi t - \theta_2) + cY_2\varpi\cos(\varpi t - \theta_2)$$

(21)
$$= Y_2\sqrt{(c\varpi)^2 + (k_2)^2}\sin(\varpi t + \beta - \theta_2)$$

where

$$\tan\beta = \frac{c\varpi}{k_2}$$

with the maximum value of $g_T(t)$ over time as,

(22)
$$(g_T)_0 = \frac{k_1 y_0 \sqrt{(c\varpi)^2 + (k_2)^2}}{\sqrt{[(k_2 - k_1) - m\varpi^2]^2 + (c\varpi)^2}}$$

3. Comparison of Computed Results

Comparing the derived equations of the transmitted force, equations 12 and 22, shows that a difference exists in the denominator of the coefficient of the sine function and also a slight difference in the expression for θ_1 and θ_2.

To facilitate comparison of the derived equations of the transmitted force, values were plugged in and the results compared using Mathcad 2000 Pro. The values used in the computation are $m = 5.1$, $k_2 = 550$, $k_1 = 1250$, $c = 21.185$, $y_0 = 25$ and $\varpi = 2.51$. Figure 6 shows the plots of the transmitted force vs. time of equations 11 and 21 superimposed on each other. Figure 7 shows the hysteresis loops.

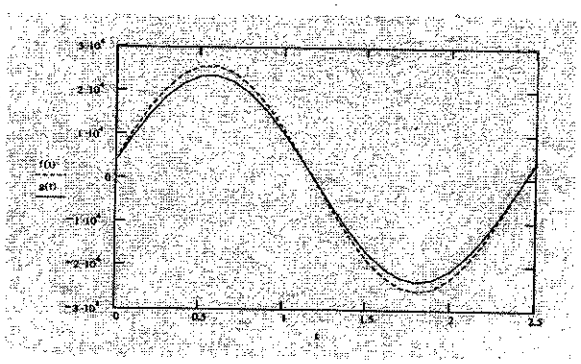

Figure 6. Transmitted Force-Time History

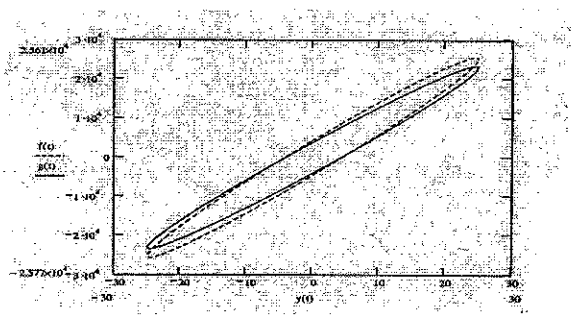

Figure 7. Hysteresis Loops

It can be seen from the plots that a variation on the transmitted force exists, an amplification occurred. Figure 7 shows the tilting of the principal axis of the hysteresis loops which can be interpreted as an increase in stiffness. From the equations derived, it can be seen that the difference in the magnitude of the force is dependent on the relative magnitudes of $(k_2 - k_1)$ and $m\varpi^2$. When $(k_2 - k_1)$ is substantially greater than $m\varpi^2$ then equations 11 and 21 are almost equal and the variation in the force is negligible. This is seen in Figure 8 which was plotted with the same values except that $k_1 = 12500$, i.e. ten times the original.

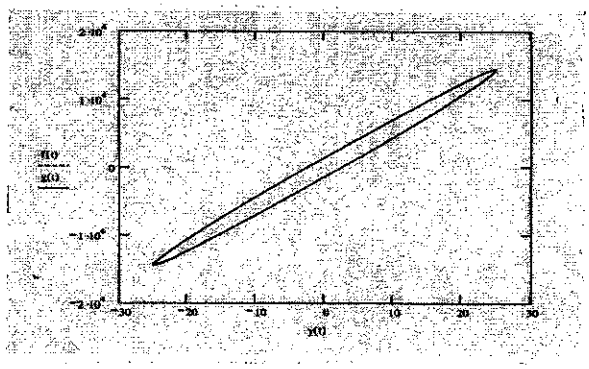

Figure 8. Hysteresis Loops

The computed values of $\theta_1 = -0.079$ and $\theta_2 = -0.073$ from the given data are almost equal such that the effect of the change in the angle is negligible. However, using Mathcad one observes that an increase in the angle θ results in an increase in the hysteresis loop area which represents the amount of energy dissipated during a cycle. Figure 9 shows the hysteresis loops for $f(t)$ when $\theta_1 = -0.2$ and $g(t)$ when $\theta_2 = -0.073$.

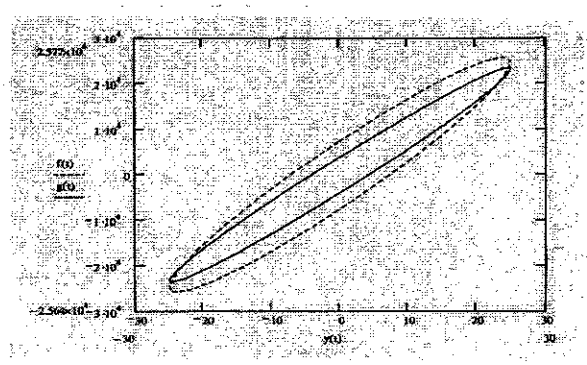

Figure 9. Hysteresis Loops

4. The Load Distribution and Energy-Dissipating Device

The LDED device is a special form of energy-dissipating device because it not only dissipates a significant amount of energy from the structure but also enhances the lateral load distribution of earthquake generated forces by effecting load sharing among the substructure components. The LDED device is especially suited for application to continuous girder bridges supported by piers having movable supports.

The LDED device allows the transfer of lateral load from the continuous girder bridge to piers having movable supports during sudden or impact loading while dissipating a portion of the energy generated especially during large earthquakes.

All these are made possible because of two major components of this device, namely: 1. the stiffening component which consists of a piston inside a cylinder housing filled with silicone putty - a material which easily deforms under slow loading but hardens when subjected to high-frequency loads, and 2. the damping component consisting of high-damping rubber vulcanized in-between two metal cylinders. Figure 10 shows the schematic of the device.

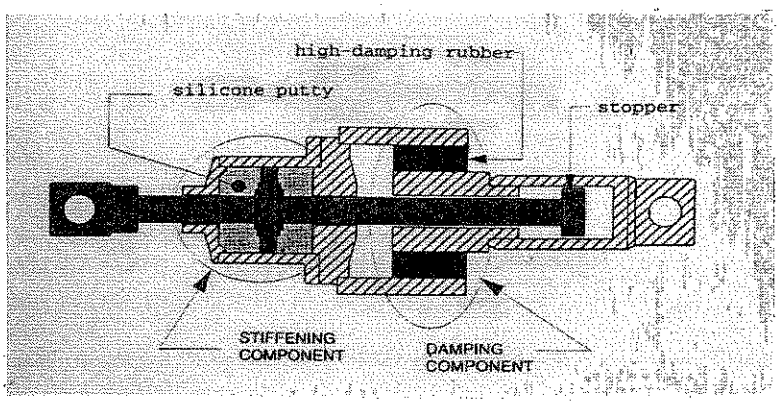

Figure 10. Load Distribution & Energy-Dissipating Device

5. Testing System

To determine the mechanical properties of LDED device, tests were made on a test rig that is capable of subjecting the device to generalized horizontal displacement-controlled and force-controlled loadings. The schematic diagram of the test set-up is shown in Figure 11.

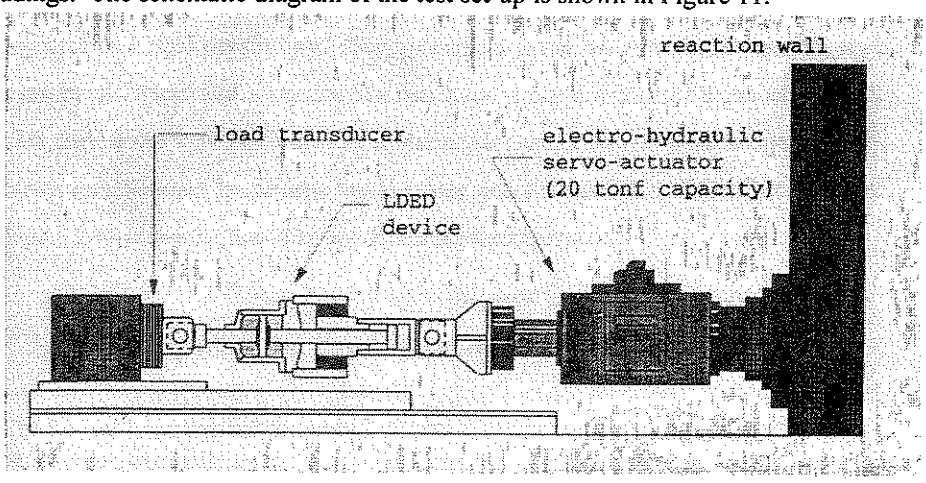

Figure 11. Schematic Diagram of Testing System

The device was rigidly connected to a load cell which measures the axial force on the system. The load cell, on the other hand, was rigidly connected to the base block. The electro-hydraulic servo-actuator which applies the axial load to the device was mounted on a rigid reaction wall. The hydraulic actuator has a maximum dynamic load capacity of 20 tonf and is capable of a maximum stroke of ± 10 cm.

6. Test Results

The device was subjected to constant amplitude displacement waves of different frequencies. The amplitude of the displacement wave was 25mm. The tests were carried out at different frequencies ranging from 0.0001 to 1.0 Hz. For a complete report on the findings regarding the behavior of the LDED device refer to the main author's thesis [Hernandez, 1998].

The hysteresis loops of the device head (end with stiffening component) and the device tail (end with the damping component) were super-imposed upon each other for comparison. Figure 12 shows the plotted hysteresis loops which reveals a behavior similar to the mass-spring-damper system model under consideration.

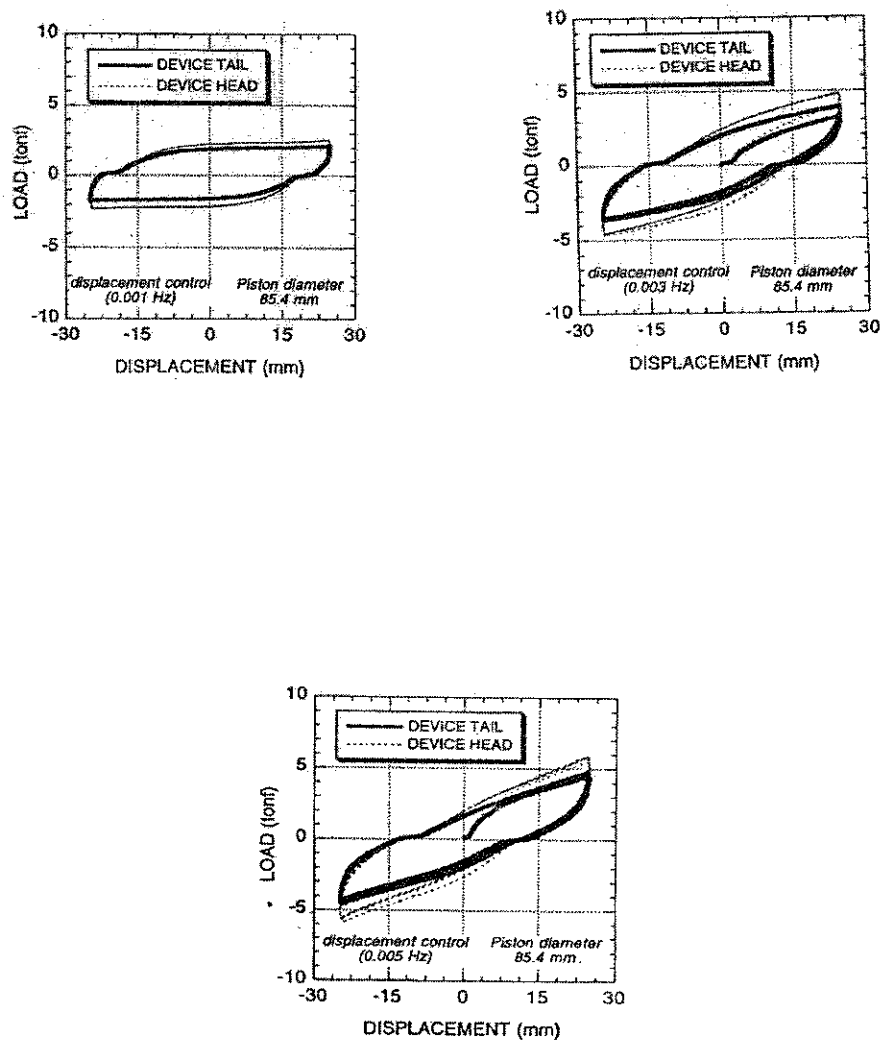

Figure 12. LDED Device Head & Device Tail Hysteresis Loops

7. Conclusion and Recommendation

The formulas derived from analysis of the mass-spring-damper system model considered in this paper showed a possible increase of the transmitted force which is clearly seen in the force-time history plots. The tilting of the hysteresis loop about its principal axis implies an increase in stiffness. The amount of increase is dependent on the relative magnitudes of $(k_2 - k_1)$, i.e. the difference in the stiffnesses of the two springs in the model, and $m\varpi^2$ - the product of the mass and the square of the frequency of loading. If $(k_2 - k_1)$ is very much greater than $m\varpi^2$ the difference in the transmitted force is negligible.

It was shown that the behavior of the LDED device observed during testing closely resembles that of the model. In other words, the mass-spring-damper system model can be used as a simplified model of the LDED device. However, there is a need for a parametric study in the determination of the stiffness k_1 which represents the effect of the stiffening component of the device. k_1 is dependent on several parameters, including the properties (in particular, the viscosity) of the silicone putty used, the frequency of loading, and the orifice size - $(R - r)$ where R is the radius of the cylinder housing and r is the radius of the piston.

8. Acknowledgement

The authors would like to express their appreciation for the support provided by Yoshifumi Uno of Kawaguchi Metal Industries Co.

9. References

Chopra, A. K. [1995]: "Dynamics of Structures - Theory and Applications to Earthquake Engineering," *Prentice Hall Inc.*

Hernandez, J. Y. Jr. [1998}: Modeling of Highly-Deformable Polymeric Damping Materials For Use in Seismic Protective Devices," *Master of Engineering Thesis*, Graduate School of Science and Engineering, Saitama University, Japan.

Paz, M. [1991]: " Structural Dynamics - Theory and Computation, 3rd Ed.," *Van Nostrand Reinhold.*

Soong, T., Dargush, G. F. [1997]: "Passive Energy Dissipation Systems in Structural Engineering," *Academic Press.*

Tanzo, W. and Tsuzuki A. [1996]: "Enhanced Seismic Lateral Load Distribution in Continuous Girder Bridges Fitted with Viscoelastic Devices," *Proceedings of the 4th International Conference on Civil Engineering, Manila.*